Development/Plasticity/Repair

The *Gli3* Hypomorphic Mutation *Pdn* Causes Selective Impairment in the Growth, Patterning, and Axon Guidance Capability of the Lateral Ganglionic Eminence

Dario Magnani,[1] Kerstin Hasenpusch-Theil,[1] Erin C. Jacobs,[2] Anthony T. Campagnoni,[2] David J. Price,[1] and Thomas Theil[1]

[1]Centre for Integrative Physiology, University of Edinburgh, Edinburgh EH8 9XD, United Kingdom, and [2]UCLA Semel Institute for Neuroscience, Los Angeles, California 90095-7332

Previous studies have defined a requirement for Sonic hedgehog (Shh) signaling in patterning the ventral telencephalon, a major source of the neuronal diversity found in the mature telencephalon. The zinc finger transcription factor Gli3 is a critical component of the Shh signaling pathway and its loss causes major defects in telencephalic development. *Gli3* is expressed in a graded manner along the dorsoventral axis of the telencephalon but it is unknown whether *Gli3* expression levels are important for dorsoventral telencephalic patterning. To address this, we used the *Gli3* hypomorphic mouse mutant *Polydactyly Nagoya* (*Pdn*). We show that in *Pdn*/*Pdn* embryos, the telencephalic expression of *Gli3* remains graded, but *Gli3* mRNA and protein levels are reduced, resulting in an upregulation of *Shh* expression and signaling. These changes mainly affect the development of the lateral ganglionic eminence (LGE), with some disorganization of the medial ganglionic eminence mantle zone. The pallial/subpallial boundary is shifted dorsally and the production of postmitotic neurons is reduced. Moreover, LGE pioneer neurons that guide corticofugal axons into the LGE do not form properly, delaying the entry of corticofugal axons into the ventral telencephalon. *Pdn*/*Pdn* mutants also show severe pathfinding defects of thalamocortical axons in the ventral telencephalon. Transplantation experiments demonstrate that the intrinsic ability of the *Pdn* ventral telencephalon to guide thalamocortical axons is compromised. We conclude that correct *Gli3* levels are particularly important for the LGE's growth, patterning, and development of axon guidance capabilities.

Introduction

The formation of a functional mammalian CNS requires the ordered generation of hundreds of different neuronal cell types. Understanding the mechanisms underlying the generation of this neuronal diversity is a major challenge in developmental neurobiology. The ventral telencephalon (VT) represents an excellent paradigm, as it gives rise not only to multiple neuronal cell types that form the basal ganglia and part of the amygdala and septum but also to several different types of olfactory and cortical interneurons. The VT also provides several cues to guide thalamocortical and corticothalamic axons (TCAs and CTAs, respectively) to their respective target areas in the cortex and thalamus.

Recent analyses have identified Sonic hedgehog (Shh) signaling as a key regulator controlling the generation of neuronal diversity in the VT. In *Shh* loss-of-function mutants, nearly all ventral telencephalic cell types are absent (Chiang et al., 1996; Rallu et al., 2002; Fuccillo et al., 2004), whereas ectopic *Shh* expression in the dorsal telencephalon results in the upregulation of ventral telencephalic markers and the downregulation of dorsal markers (Ericson et al., 1995; Shimamura and Rubenstein, 1997; Kohtz et al., 1998; Gaiano et al., 1999; Rallu et al., 2002). Similarly, Gli transcription factors, critical components of the Shh signaling pathway, are required for telencephalic development. Mutations in *Gli3*, in particular, affect the development of both ventral and dorsal components of the telencephalon (Grove et al., 1998; Theil et al., 1999; Tole et al., 2000; Kuschel et al., 2003; Theil, 2005; Fotaki et al., 2006; Friedrichs et al., 2008; Quinn et al., 2009; Yu et al., 2009a). In the dorsal telencephalon, *Gli3* controls patterning independently of *Shh*, but in the VT, *Gli3* transcription and cleavage of Gli3 protein into its repressor form are suppressed by Shh signaling, resulting in a dorsal^{high} to ventral^{low} gradient of *Gli3* expression. Ventral telencephalic patterning is restored in *Shh*;*Gli3* double mutants, suggesting that *Shh* and *Gli3* act antagonistically to pattern the VT (Aoto et al., 2002; Rallu et al., 2002; Rash and Grove, 2007). It remains unclear, however, as to what extent the dorsoventral gradient of *Gli3* expression is important for dorsoventral telencephalic patterning. As this question cannot be addressed in the *Gli3*-null mutant *extra-toes*, we used the *Gli3* hypomorphic mouse mutant *Polydactyly Nagoja* (*Pdn*) (Hayasaka et al., 1980). We show that in *Pdn*/*Pdn* mutants, levels of *Gli3* mRNA and protein are reduced in the VT whereas the overall *Gli3* expression pattern remains unaltered, resulting in a shallower gradient of *Gli3* expression. This change causes an upregulation of *Shh* expression and signaling in the VT and se-

Received July 14, 2010; revised Aug. 13, 2010; accepted Aug. 22, 2010.

This work was supported by a grant from the Deutsche Forschungsgemeinschaft (TH770/6-1) and from the Medical Research Council. We thank Drs. Thomas Becker, Vassiliki Fotaki, John Mason, and Tom Pratt for critical comments on the manuscript. We are grateful to Manuel Valiente in Oscar Marin's lab for teaching the transplantation technique and Oscar Marin and Kenneth Campbell for providing *in situ* hybridization probes and antibodies.

Correspondence should be addressed to Thomas Theil at the above address. E-mail: thomas.theil@ed.ac.uk.

DOI:10.1523/JNEUROSCI.3650-10.2010

 0270-6474/10/3013883-12$15.00/0

verely affects the development of the lateral ganglionic eminence (LGE), which becomes ventralized at caudal levels and produces fewer neurons. The formation of the pallial/subpallial boundary (PSPB) is defective and corticothalamic and thalamocortical tracts show severe axon-guidance defects. Transplantation experiments show that the axon-guidance defects are caused at least in part by abnormalities intrinsic to the VT.

Materials and Methods

Mice. Pdn heterozygous animals were kept on a C3H/He background and were interbred. Embryonic (E) day 0.5 was assumed to start at midday of the day of vaginal plug discovery. Embryos were genotyped as described previously (Ueta et al., 2002). In qualitative analyses of mutant phenotypes, heterozygous and wild-type embryos did not show differences and both were used as control embryos. For quantitative analyses, wild-type and *Pdn*/*Pdn* embryos were compared to avoid the possible risk of *Pdn*/+ embryos having subtle defects. For each marker and each stage, three to five non-exencephalic embryos were analyzed at rostral, medial, and caudal levels of the developing forebrain. Golli-τGFP (Jacobs et al., 2007) and τGFP mice (Pratt et al., 2000) were bred into the *Pdn* line.

In situ *hybridization and immunohistochemistry.* Antisense RNA probes for *Dbx1* (Yun et al., 2001), *Dlx2* (Bulfone et al., 1993), *Ebf1* (López-Bendito et al., 2006), *Gli1* (Hui et al., 1994), *Gsh1* (Valerius et al., 1995), *Nkx2.1* (Lazzaro et al., 1991), *Nkx6.2* (Qiu et al., 1998), *Ptc* (Goodrich et al., 1996), *Shh* (Echelard et al., 1993), and *Six3* (Oliver et al., 1995) were labeled with digoxigenin. *In situ* hybridization on 12 μm serial paraffin sections of mouse embryos were performed as described previously (Theil, 2005).

Immunohistochemical analysis was performed as described previously (Theil, 2005) using antibodies against the following molecules: bromodeoxyuridine (BrdU, 1:50; Abcam), BrdU and iododeoxyuridine (IdU, 1:50; BD Bioscience), green fluorescent protein (GFP, 1:1000; Abcam), Glast (1:5000, Chemicon), Gsh2 (1:2500) (a gift from K. Campbell, Cincinnati Children's Hospital Medical Center, Cincinnati, OH), Isl1/2 (1:100; DSHB), neurofilament (1:5; DSHB), Pax6 (1:100; DSHB), PCNA (1:500; Abcam), phosphohistone-H3 (1:1000; Millipore), and β-III-tubulin (Tuj1 antibody, 1:1000; Sigma).

For measuring cell cycle lengths, pregnant females received a single, intraperitoneal injection of IdU (10 mg/ml) at E10.5, followed by an injection of BrdU 90 min later. Embryos were collected 2 h after the initial injection. To determine the generation of neurons by pulse-chase experiments, E10.5 pregnant females were intraperitoneally injected with BrdU. Embryos were harvested 24 h later and stained for BrdU and PCNA. The fraction of cells in the LGE and medial ganglionic eminence (MGE) that had left the cell cycle and differentiated into neurons was calculated by dividing the number of $BrdU^+$ $PCNA^-$ cells by the total number of $BrdU^+$ cells.

Carbocyanine dye injection and analysis. Brains were fixed overnight in 4% (w/v) paraformaldehyde (PFA) at 4°C. For cortical injections, single crystals of the lipophilic tracer DiI were injected into the cortex of whole brains at three or four symmetrical positions along the rostrocaudal extent of the cortex using pulled-glass capillaries. For thalamic injections, caudal parts of the brains were removed with a coronal cut to expose the caudal surface of the dorsal thalamus. Depending on brain size, single crystals were injected at one to three positions along the dorsoventral extent of the dorsal thalamus. Dyes were allowed to diffuse at room temperature for 4–8 weeks in 4% (w/v) PFA in PBS. Brains were rinsed in PBS, embedded in agarose, and sectioned coronally on a vibratome at 100–200 μm. Sections were cleared in 9:1 glycerol:PBS solution containing the nuclear counterstain TOPRO3 (0.2 μM) overnight at 4°C.

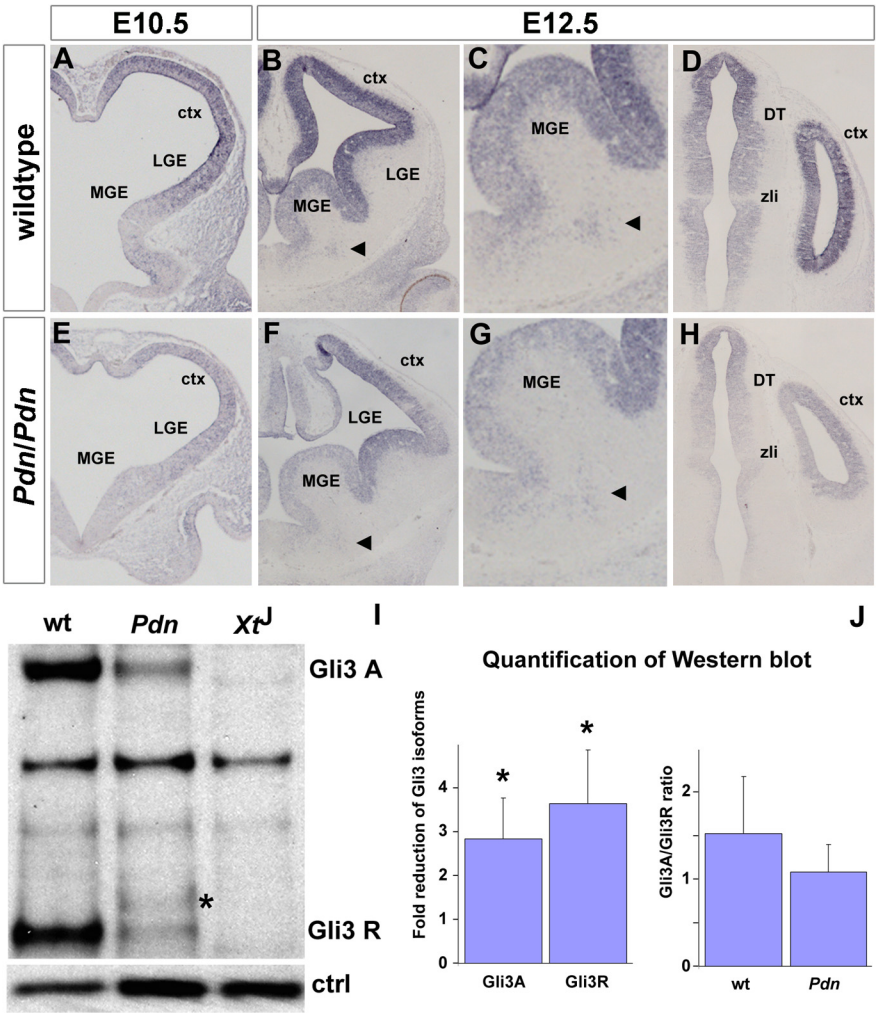

Figure 1. *Gli3* expression is reduced in the forebrain of *Pdn*/*Pdn* mutants. ***A–H***, *Gli3 in situ* hybridization on coronal sections through the forebrain of E10.5 (***A***, ***D***) and E12.5 (***B***, ***C***, ***E***, ***F***) wild-type (wt; ***A–C***) and *Pdn*/*Pdn* (***D–F***) embryos. *Gli3* mRNA levels are clearly reduced in *Pdn* mutants but the overall expression pattern is conserved. The arrowheads in ***B***, ***C***, ***F***, and ***G*** mark *Gli3* expression in the MGE mantle zone. ***I***, Gli3 Western blot analysis with E12.5 ventral telencephalic extracts. In *Pdn* mutant extract, Gli3 activator and repressor forms are present at reduced level but are absent in Xt^J mutants. The asterisk indicates an additional Gli3-specific 85 kDa protein. An unspecific 50 kDa band was used as a loading control. ***J***, Quantification of Western blot data. Asterisk (*) denotes statistically significant changes with $p \leq 0.05$. ctx, Cortex; DT, dorsal thalamus; zli, zona limitans intrathalamica.

Explant culture. Organotypic slice cultures of different levels of the embryonic mouse telencephalon were prepared as previously described (López-Bendito et al., 2006). Brain slices were cultured on polycarbonate culture membranes (8 μm pore size; Corning Costar) in organ-tissue dishes containing 1 ml of medium [Neurobasal/B-27 (Invitrogen) supplemented with glutamine, glucose, penicillin, and streptomycin]. Slices were cultured for 72 h, fixed with 4% PFA, and processed for anti-GFP immunofluorescence as described above.

Quantitative reverse transcription PCR. cDNA samples were collected from the E10.5 telencephalon and from the E12.5 VT of wild-type or *Pdn*/*Pdn* embryos. Quantitative reverse transcription PCR (qRT-PCR) used the following primer pairs: *Shh* (5′-ATTTTGTGAGGCCAAGCAAC-3′ and 5′-CAGGAGCATAGCAGGAGAGG-3′), *Gli1* (5′-GTTATGGAGCAGCCAGAGAG-3′ and 5′-GAGTTGATGAAAGCCACCAG-3′), *Ptc1* (5′-GCATTCTGGCCCTAGCAATA-3′ and 5′-CAACAGTCAC-

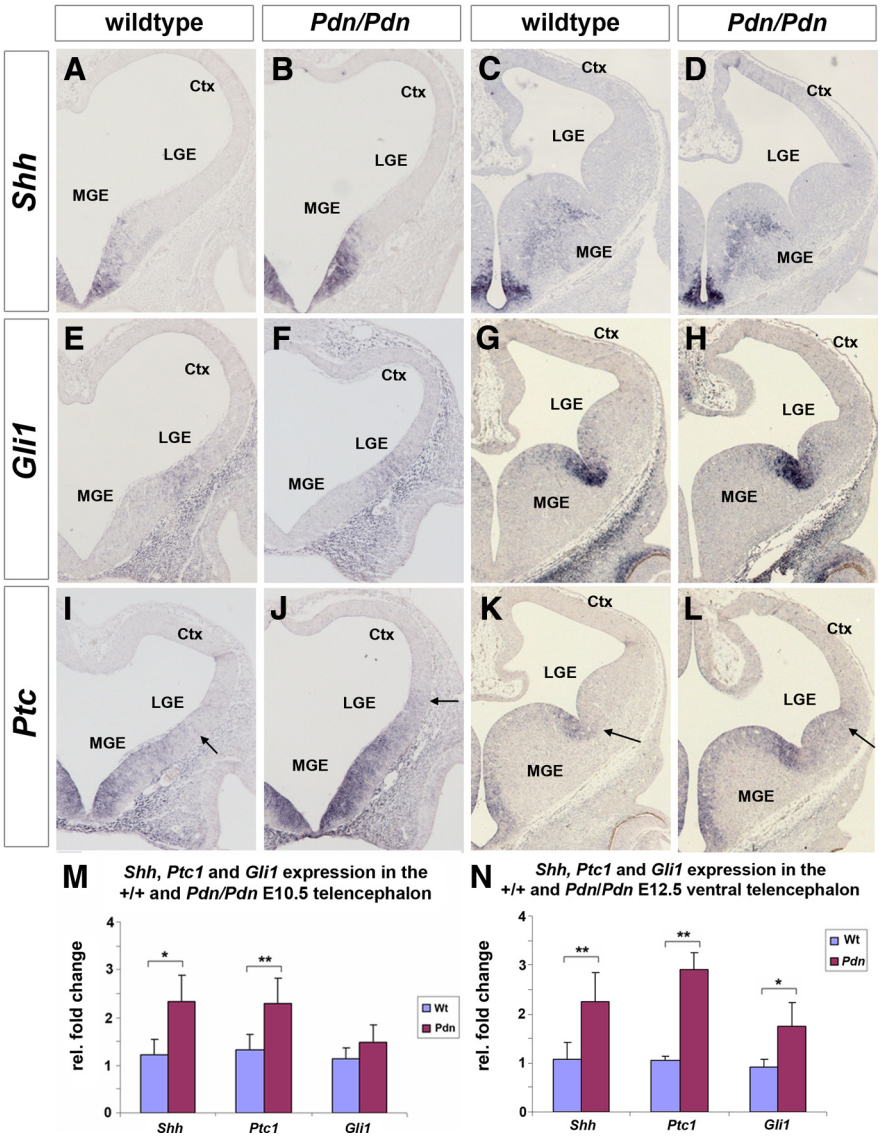

Figure 2. Upregulation of *Shh* expression and signaling in the VT of *Pdn/Pdn* mutants. ***A–L***, Coronal sections through the forebrain of E10.5 (***A***, ***B***, ***E***, ***F***, ***I***, ***J***) and E12.5 (***C***, ***D***, ***G***, ***H***, ***K***, ***L***) embryos hybridized with the indicated probes. (***A–D***) *Shh* expression is increased but remains confined to the MGE of *Pdn* mutants. ***E–H***, *Gli1* expression remains restricted to the interganglionic sulcus. ***I–L***, *Ptc1* expression is upregulated and extends into the LGE of E12.5 *Pdn/Pdn* embryos. Arrows mark the dorsal boundary of Ptc1 expression. ***M***, ***N***, qRT-PCR analysis of *Shh*, *Gli1*, and *Ptc1* expression in the E10.5 telencephalon (***M***) and E12.5 ventral telencephalon (***N***). Asterisks (* and **) denote statistically significant changes with $p \leq 0.05$ and $p \leq 0.001$, respectively. ctx, Cortex; wt, wild type.

CGAAGCAGAA-3′), and *Gapdh* (5′-AGGTTGTCTCCTGCGACTTCA-3′ and 5′-CCAGGAAATGAAGCTTGACAAAG-3′). qRT-PCR was performed using Quantitect SYBR Green PCR kit (Qiagen) and a DNA Engine Opticon System (GRI). The abundance of each transcript in the original RNA sample was extrapolated from PCR kinetics using Opticon software.

Western blotting. Protein was extracted from VT of E12.5 wild-type and *Pdn/Pdn* embryos as described previously (Fotaki et al., 2006). Equivalent amounts of protein were subjected to gel electrophoresis on a 3–8% gradient Tris-acetate gel (Invitrogen), and protein was transferred to a nitrocellulose membrane, which was incubated with rabbit polyclonal anti-Gli3 antibody (1:500; Abcam). After incubating with a horseradish peroxidase-conjugated anti-rabbit IgG secondary antibody (1:2000; Dako), signal was detected using ECL Plus detection (GE Healthcare). Band intensity was measured using ImageJ software and was normalized for the loading control.

Results

Shh signaling is upregulated in the VT of *Pdn/Pdn* mutants

To test the effect of the *Pdn* mutation on *Gli3* expression, we performed *in situ* hybridizations on coronal sections of the E10.5 and E12.5 forebrain. Confirming previous findings, *Gli3* transcripts are restricted mainly to the ventricular zones of the developing cortex, VT, and thalamus of wild-type embryos (Fig. 1*A–D*) (Hui et al., 1994; Fotaki et al., 2006). In the VT, *Gli3* shows a lateral^{high} to medial^{low} gradient of expression with low expression levels in the MGE. Upon longer color development, we also noted a previously undescribed group of *Gli3*-expressing cells in the MGE mantle (Fig. 1*C*). In *Pdn/Pdn* mutant embryos, this expression pattern is conserved, although overall *Gli3* expression levels are clearly reduced (Fig. 1*E–H*).

Reduced Gli3 expression was also evident at the protein level (Fig. 1*I*). In protein extracts from the E12.5 VT of wild-type embryos, Western blots using a Gli3 *N*-terminal antibody showed two Gli3 forms of 170 and 80 kDa, corresponding to the Gli3 activator and repressor, respectively. In *Pdn/Pdn* mutants, both forms are present but are reduced approximately threefold (repressor, 3.6-fold ± 1.2 SEM; activator, 2.8-fold ± 0.9; $n = 5$). Interestingly, the ratio of Gli3 repressor to activator remains unaltered (wild-type, 1.5 ± 0.7 compared with 1.1 ± 0.3 for *Pdn/Pdn*; $n = 3$). This analysis also revealed low amounts of an additional *Pdn/Pdn*-specific Gli3 protein of ~85 kDa (Fig. 1*I*, asterisk), which is likely to be encoded by previously described alternative splice products, leading to the insertion of 56 or 61 aa in the *N*-terminal part of the Gli3 protein (Thien and Rüther, 1999; Ueta et al., 2002). The presence of a Gli3 activator protein containing the same additional amino acids is likely, but could not be resolved on these gels due to its high molecular weight (170 kDa compared with 175 kDa). Together, these analyses revealed reduced expression levels of *Gli3* mRNA and protein while the overall *Gli3* expression pattern and in particular its graded expression in the VT is not affected by the *Pdn* mutation.

We next analyzed whether the *Pdn* mutation alters Shh signaling in the VT by determining *Shh* expression and that of its target genes, *Gli1* and *Ptc1* (Goodrich et al., 1996; Lee et al., 1997), at E10.5 and E12.5. In wild-type embryos, *Shh* expression was confined to MGE progenitor cells and to the MGE mantle zone at E10.5 and E12.5, respectively (Fig. 2*A*,*C*); *Gli1* was expressed in the progenitor cells at the interganglionic sulcus separating the LGE and MGE (Fig. 2*E*,*G*); and *Ptc1* was expressed in the ventricular zone of the E10.5 and E12.5 MGE (Fig. 2*I*,*K*). In *Pdn/Pdn* brains, patterns of expression were similar, but the domain of *Ptc1* was expanded dorsally and overall expression levels of at least *Shh* and *Ptc1* might be increased (Fig. 2*B*,*D*,*F*,*H*,*J*,*K*). Expression levels were therefore quantified by qRT-PCR on dissected E10.5 whole telencephali and on E12.5 ventral telencephali (Fig. 2*M*,*N*). This showed an approximately twofold increase in

Shh and *Ptc1* expression levels at both ages whereas *Gli1* expression levels were significantly upregulated only at E12.5. Together, these experiments show an upregulation of *Shh* expression and increased Shh signaling in the mutant E10.5 and E12.5 VT.

The *Pdn/Pdn* VT displays patterning defects

We next tested whether the alterations in *Gli3* expression and Shh signaling described above might affect dorsoventral telencephalic patterning. To delineate the boundary between the dorsal and ventral telencephalon, we examined *Dlx2* and Gsh2 expression. *Dlx2* is expressed throughout the proliferative zone of the ventral telencephalon (Fig. 3*A*), whereas Gsh2 is expressed in a dorsal^{high} to ventral^{low} gradient in the LGE (Fig. 3*C*). Both markers show a sharp expression boundary at the PSPB. In *Pdn/Pdn* brains, *Dlx2* and Gsh2 expression are maintained in the VT but expand more dorsally. At the PSPB, some *Dlx2*$^+$ cells intermingle with *Dlx2*$^-$ cells and some Gsh2$^+$ cells are mixed with Gsh2$^-$ cells, suggesting abnormalities in the establishment or maintenance of this boundary (Fig. 3*B*,*D*). These findings were confirmed by the expression of markers characteristic of the dorsal telencephalon. In control embryos, Pax6 expression is detected at high levels in neocortical progenitors with a sharp expression boundary at the PSPB (Fig. 3*E*). In *Pdn/Pdn* mutants, the ventral limit of this expression at the PSPB is shifted dorsally closer to the angle region at the most lateral end of the LGE (Fig. 3*F*). The Pax6-expressing corticostriatal stream that emanates from the PSPB region is severely reduced in mutant embryos (Fig. 3*E*,*F*). Similarly, the expression of *Dbx1*, which is confined to progenitor cells of the ventral pallium (i.e., the region dorsal to the PSPB) of control embryos (Yun et al., 2001) (Fig. 3*G*), is shifted dorsally in the *Pdn/Pdn* telencephalon and expands into more dorsal regions of the neocortex (Fig. 3*G*,*H*) as in other *Gli3* mutants (Hanashima et al., 2007; Friedrichs et al., 2008). These marker analyses indicate that the boundary between ventral and dorsal telencephalon is defective, with the PSPB becoming less defined and shifted dorsally in *Pdn/Pdn* mutants.

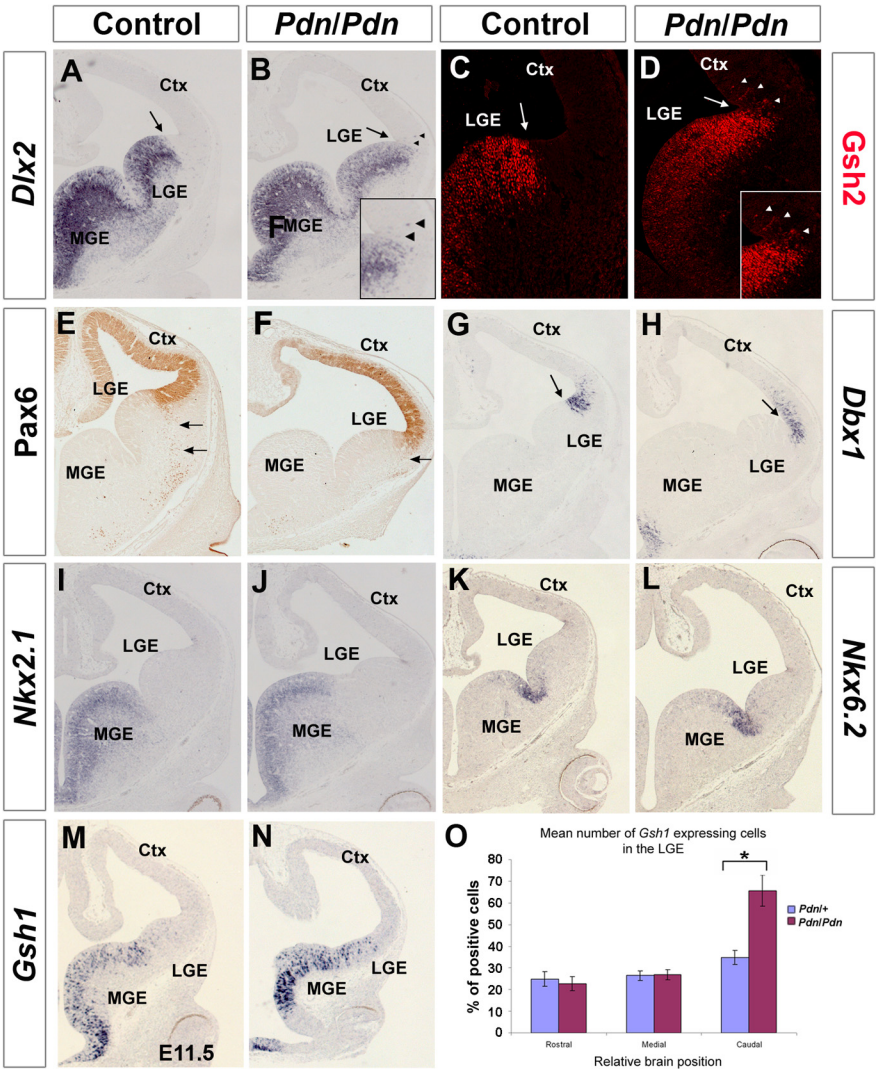

Figure 3. Regionalization defects in the VT of *Pdn/Pdn* embryos. ***A–N***, *In situ* hybridization (***A***, ***B***, ***G–N***) and immunostainings (***C–F***) on E12.5 coronal sections with the indicated probes and antibodies. ***A–D***, Stainings for *Dlx2* (***A***, ***B***) and Gsh2 (***C***, ***D***) define the PSPB (arrows), which is shifted dorsally. Note the scattered Dlx2-expressing and Gsh2$^+$ cells in neocortical territory in *Pdn* mutants (arrowheads). ***E***, In control embryos, Pax6 expression sharply abuts the PSPB and marks the migrating cells of the corticostriatal stream. ***F***, In *Pdn/Pdn* mutants, the ventral Pax6 expression boundary is shifted dorsally and the corticostriatal stream is severely reduced (arrow). ***G***, ***H***, *Dbx1* expression, which is characteristic of the ventral pallium in control embryos, is shifted dorsally in *Pdn* mutants and expands further into the neocortex. ***I–L***, *Nkx2.1* and *Nkx6.2* expression define the extent of the MGE. ***M***, ***N***, *Gsh1* expression is mainly restricted to the MGE of control embryos (***M***) but expands into the dorsal LGE of *Pdn* mutants (***N***). ***O***, Quantification of the numbers of *Gsh1*-expressing cells in the LGE. Asterisk (*) denotes statistically significant changes with $p \leq 0.05$. ctx, Cortex.

Next, we analyzed the molecular regionalization within the *Pdn/Pdn* VT. Based upon their expression profiles, LGE and MGE progenitor regions can be subdivided into molecular subterritories (Yun et al., 2001; Flames et al., 2007). *Nkx2.1* expression is confined to the MGE, whereas *Nkx6.2* is expressed on either side of the interganglionic sulcus (Fig. 3*I*,*K*). No differences were found in the expression of either marker in *Pdn/Pdn* brains, suggesting that the subdivision of the ventral telencephalon in LGE and MGE is not affected (Fig. 3*J*,*L*). The *Gsh1* homeobox gene is expressed in a "salt and pepper" fashion at high levels in the MGE and at lower levels in the ventral LGE but not in the dorsal LGE (Yun et al., 2003) (Fig. 3*M*). In *Pdn/Pdn* mutants, *Gsh1* expression extends into the dorsal LGE but only at caudal levels. To quantify this effect, we subdivided the LGE where it was anatomically and molecularly (lack of *Nkx2.1* expression) distinct from the MGE into rostral, central, and caudal regions but excluded the caudal-most telencephalon containing the caudal ganglionic eminence. Counting *Gsh1*-expressing cells in the so-defined LGE showed a approximately twofold increase in the number of *Gsh1*-expressing cells specifically in the caudal LGE (Mann–Whitney test, $p = 0.034$, $n = 3$) (Fig. 3*O*), suggesting a partial ventralization of the *Pdn/Pdn* caudal LGE.

During this marker analysis, we noticed that the *Pdn/Pdn* LGE appears smaller and does not protrude as much into the ventricle as in controls. The thickness of the proliferative region of the *Pdn/Pdn* LGE does not seem to be affected, but the mantle region containing postmitotic neurons seemed to be thinner (Fig. 3). We

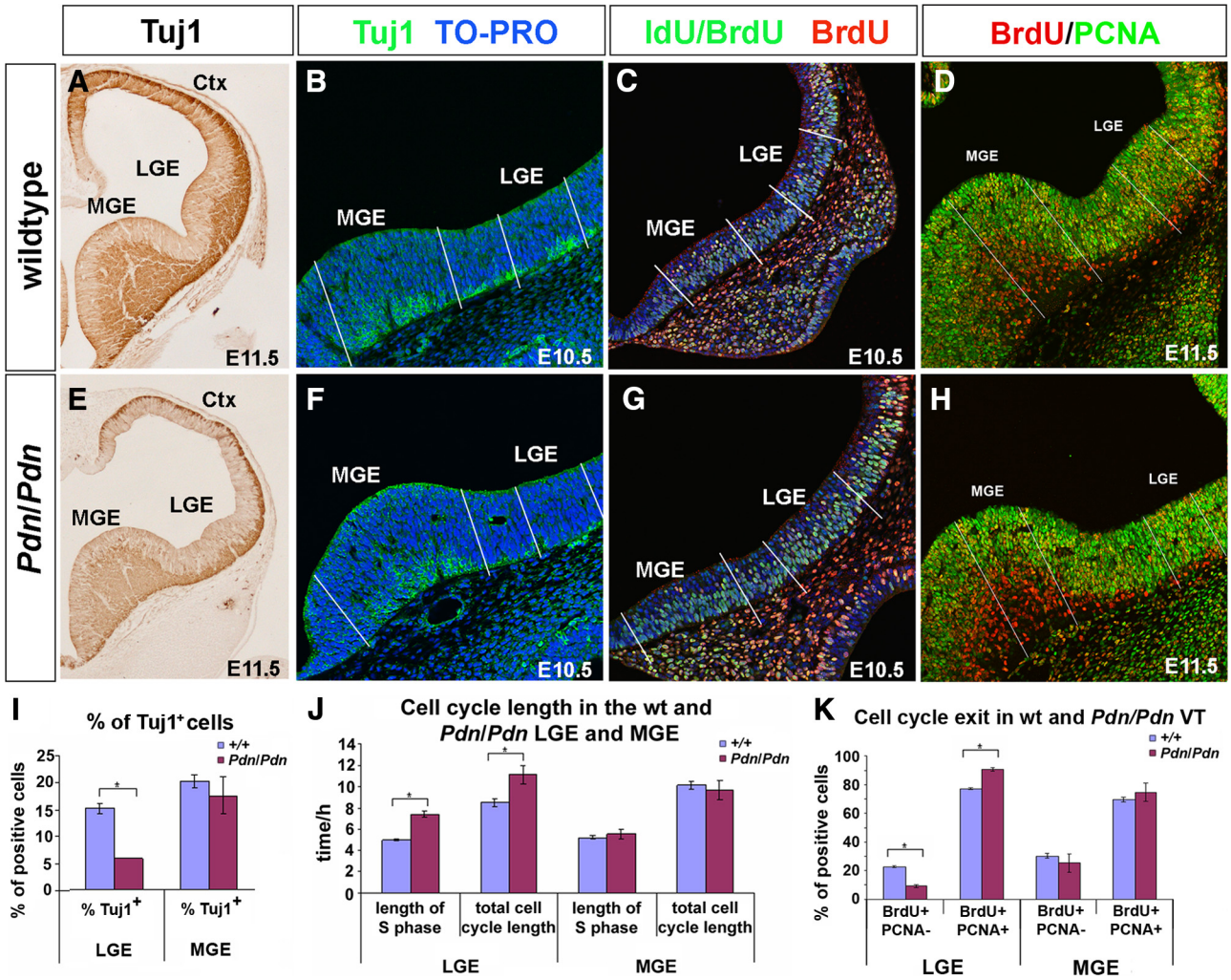

Figure 4. Diminished neuronal differentiation in the *Pdn* mutant LGE. ***A–H***, Coronal sections through the forebrain of E11.5 (***A***, ***D***, ***E***, ***H***) and E10.5 (***B***, ***C***, ***F***, ***G***) embryos were stained with the indicated antibodies. ***A***, ***E***, The LGE neuronal layer is reduced in size and has similar sizes in the MGE and preplate. ***B***, ***F***, The E10.5 LGE of *Pdn* mutants generates fewer neurons. ***C***, ***G***, BrdU/IdU immunostaining to determine total cell cycle length and S-phase length of neural precursors in the LGE and MGE. ***D***, ***H***, BrdU (injected at E10.5) and PCNA staining reveal the fraction of cells leaving the cell cycle and differentiating into neurons in the LGE and MGE. ***I***, Quantification of Tuj1 $^{+}$ cells in the VT of wild-type (wt) and *Pdn/Pdn* E10.5 embryos. ***J***, Quantification of the cell cycle length in the wild-type and *Pdn* mutant E10.5 telencephalon. ***K***, Quantification of the fraction of cells leaving the cell cycle (BrdU $^{+}$/PCNA $^{-}$) and of cycling progenitors (BrdU $^{+}$/PCNA $^{+}$) in wild-type and *Pdn* mutant embryos. Asterisk (*) denotes statistically significant changes with $p \leq 0.05$. ctx, Cortex.

therefore tested the *Pdn/Pdn* VT for its ability to produce neurons at early steps of forebrain development by Tuj1 immunohistochemistry, an early panneuronal marker. In control embryos, this staining revealed thick MGE and LGE mantle regions and the preplate overlying the cortical ventricular zone (Fig. 4*A*). In *Pdn/Pdn* embryos, we found no differences in Tuj1 expression in the MGE mantle or in the preplate, but the LGE mantle region appeared thinner, suggesting a defect in neurogenesis (Fig. 4*E*). To define the origin of this defect, Tuj1 staining was repeated on E10.5 telencephali (Fig. 4*B*,*F*). On adjacent sections, *Nkx2.1* and *Dlx2 in situ* hybridizations were used to identify LGE and MGE (data not shown). Tuj1 $^{+}$ cells were then counted in LGE and MGE territories. Although this analysis did not reveal significant differences in the percentage of Tuj1 $^{+}$ cells between wild-type and *Pdn/Pdn* MGE, the percentage of Tuj1 $^{+}$ cells within the *Pdn/Pdn* LGE was significantly reduced to approximately one-third (Fig. 4*I*) (Mann–Whitney test, $p = 0.05$, $n = 3$), suggesting that the size reduction of the *Pdn/Pdn* LGE results from a reduced number of postmitotic neurons.

This reduction may be explained by a reduced number of dividing cells or by an increase in apoptosis. However, the proportions of neither mitotic nor apoptotic cells appeared altered in the *Pdn/Pdn* LGE (supplemental Fig. 1, available at www.jneurosci.org as supplemental material). Alternatively, the *Pdn* mutation may alter the cell cycle parameters of LGE progenitors. A BrdU/IdU labeling strategy (Martynoga et al., 2005) was used to determine the total cell cycle length (T_L) and the length of the S phase (T_S) in the ventral telencephalon of wild-type and *Pdn/Pdn* E10.5 brains (Fig. 4*C*,*G*). We found no differences in either T_S or T_L of MGE progenitors (Fig. 4*J*). However, in proliferating cells of the mutant LGE, T_S and T_L were significantly longer by ~2 and 2.5 h, respectively (Mann–Whitney test, $p = 0.05$, $n = 3$), suggesting that *Pdn/Pdn* LGE proliferating cells progress through the cell cycle at a slower rate. To further address whether the generation of neurons is modified in the LGE, we performed BrdU pulse chase experiments. BrdU was given to E10.5 pregnant mice 24 h before dissection at E11.5 and PCNA staining was used to reveal all proliferating cells. This analysis showed that the fraction of cells leaving the cell cycle and differentiating into neurons (BrdU $^{+}$/PCNA $^{-}$) is significantly reduced in the LGE of *Pdn/Pdn* mutants, whereas the fraction of progenitors (BrdU $^{+}$/PCNA $^{+}$)

is significantly increased. In contrast, the *Pdn* mutation did not affect the generation of neurons in the MGE (Fig. 4*D*,*H*,*K*). Together, these data suggest that the reduction in the size of the LGE is due to a reduced number of Tuj1$^+$ postmitotic neurons. As the *Pdn* mutation selectively increases the cell cycle length of LGE precursor cells, this elongation is likely to contribute to a reduced differentiation rate in the mutant LGE.

The *Pdn* mutation affects the formation of ventral telencephalic structures important for the guidance of thalamocortical and corticothalamic axons

We next addressed how later development of the *Pdn*/*Pdn* VT is affected. The LGE plays prominent roles in the guidance of TCA and CTA to their target areas in the cortex and thalamus, respectively. We therefore analyzed whether the formation of cues that guide these axons is affected in *Pdn*/*Pdn* embryos.

Initially, the LGE and the MGE provide two different transient populations of pioneer neurons that send their axons toward the cortex and thalamus, respectively (Métin and Godement, 1996; Molnár et al., 1998; Tuttle et al., 1999). These pioneer axons act as a scaffold on which CTAs and TCAs enter the VT. Since no markers are available to selectively label these neurons, we investigated the presence of MGE and LGE pioneers in *Pdn*/*Pdn* embryos by DiI injections into the E12.5 thalamus and neocortex. In control embryos, these injections retrogradely label axons projecting from MGE and LGE pioneer neurons and their cell bodies ($n = 4$ for each label) (Fig. 5*A*–*D*). Similarly, DiI injections into the *Pdn*/*Pdn* thalamus labeled the MGE pioneers in the mutant ($n = 4$) (Fig. 5*E*,*F*). In contrast, DiI injected in the E12.5 cortex of *Pdn*/*Pdn* mutants did not reveal any pioneer cell bodies and axons in the LGE in any of the four brains that were analyzed (Fig. 5*G*,*H*). These data suggest that MGE pioneer neurons are present, but LGE pioneer neurons either fail to project toward the cortex or are absent in *Pdn* mutants.

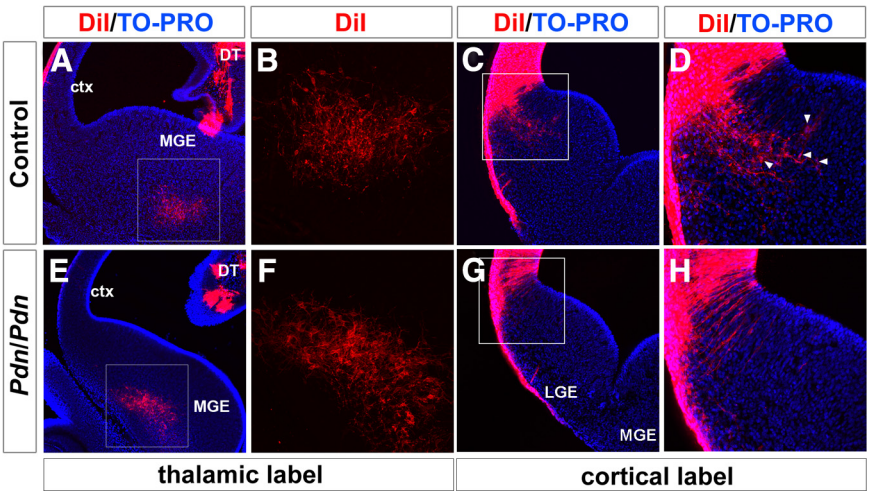

Figure 5. LGE pioneer neurons cannot be retrogradely labeled by cortical DiI injections. ***A***, ***B***, ***E***, ***F***, DiI injections into the E12.5 thalamus retrogradely label pioneer neurons in the MGE of control and *Pdn*/*Pdn* embryos. ***C***, ***D***, ***G***, ***H***, DiI injections into the E12.5 back-label LGE pioneer neurons in the control LGE but not in *Pdn*/*Pdn* mutants. ctx, Cortex; DT, dorsal thalamus.

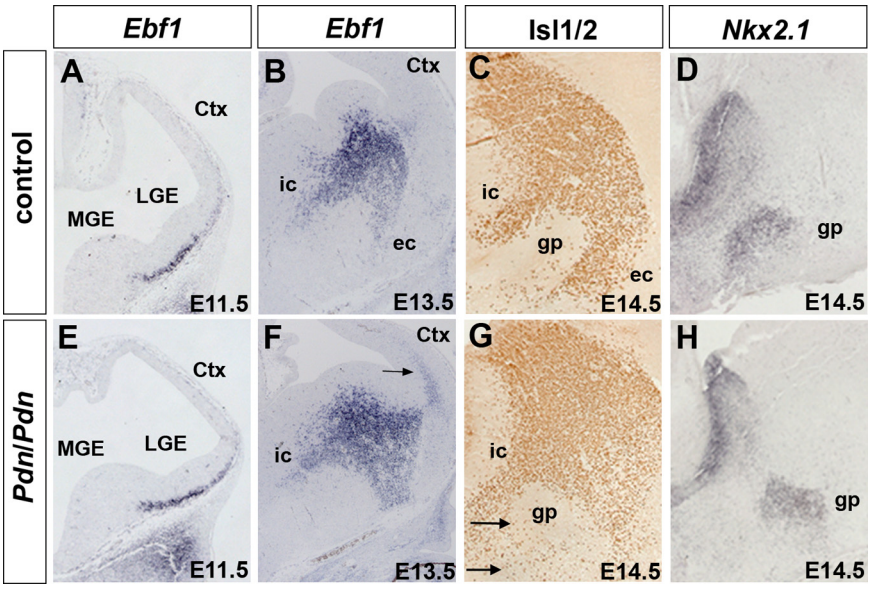

Figure 6. Formation of the ventral telencephalic corridor in the *Pdn* mutant VT. ***A***–***H***, Coronal sections through the VT of control (***A***–***D***) and *Pdn* mutant embryos (***E***–***H***) hybridized with the indicated probes. ***A***, ***E***, *Ebf1* expression marks future corridor cells from their site of origin in the LGE in E11.5 control and *Pdn* mutant embryos. ***B***, ***F***, In E13.5 control embryos, *Ebf1*-expressing cells settle dorsal and ventral to the globus pallidus corresponding to the internal (ic) and external (ec) capsule, respectively. In *Pdn* mutants, the external capsule does not form properly. ***C***, ***G***, Isl1/2 immunohistochemistry revealing the distribution of corridor cells. Isl1/2$^+$ cells are more dispersed in the MGE mantle of *Pdn*/*Pdn* embryos. ***D***, ***H***, *Nkx2.1 in situ* hybridization labels MGE progenitor cells and the globus pallidum (gp), which has an abnormal size in *Pdn* mutants. ctx, Cortex.

Recent analysis has shown that cells originating in the LGE migrate into the MGE and form a permissive corridor along which TCAs traverse the MGE (López-Bendito et al., 2006). Corridor cells are marked by *Ebf1* expression from their birth in the E11.5 LGE and during their migration into the MGE, where they settle dorsal and ventral to the globus pallidus with the upper branch corresponding to the corridor and the lower branch to the external capsule (Fig. 6*A*,*B*) (López-Bendito et al., 2006). In *Pdn*/*Pdn* embryos, *Ebf1*-expressing cells are formed in the LGE (Fig. 6*E*) and migrate toward the MGE, but their final organization in the MGE is altered (Fig. 6*F*). Although the corridor forms in mutant embryos, *Ebf1*-positive cells were not detected in a position ventral to the globus pallidus but in a broad stream extending toward the pial surface (Fig. 6*F*). Cells expressing *Ebf1* weakly are also present ectopically in mutant dorsal telencephalon (Fig. 6*F*, arrow). This abnormality in the MGE mantle region was confirmed by staining for Isl1/2, which marks cells in both the internal and the external capsule in wild-type embryos. In *Pdn*/*Pdn* embryos, Isl1/2$^+$ cells were only detected dorsally of the globus pallidus (Fig. 6*C*,*G*). This analysis also revealed a number of scattered Isl1/2$^+$ cells medial to the globus pallidus in the ventromedial MGE (Fig. 6*G*, arrows), which were not detected in control embryos. *Nkx2.1* staining on adjacent sections also showed that the globus pallidus (López-Bendito et al., 2006) is

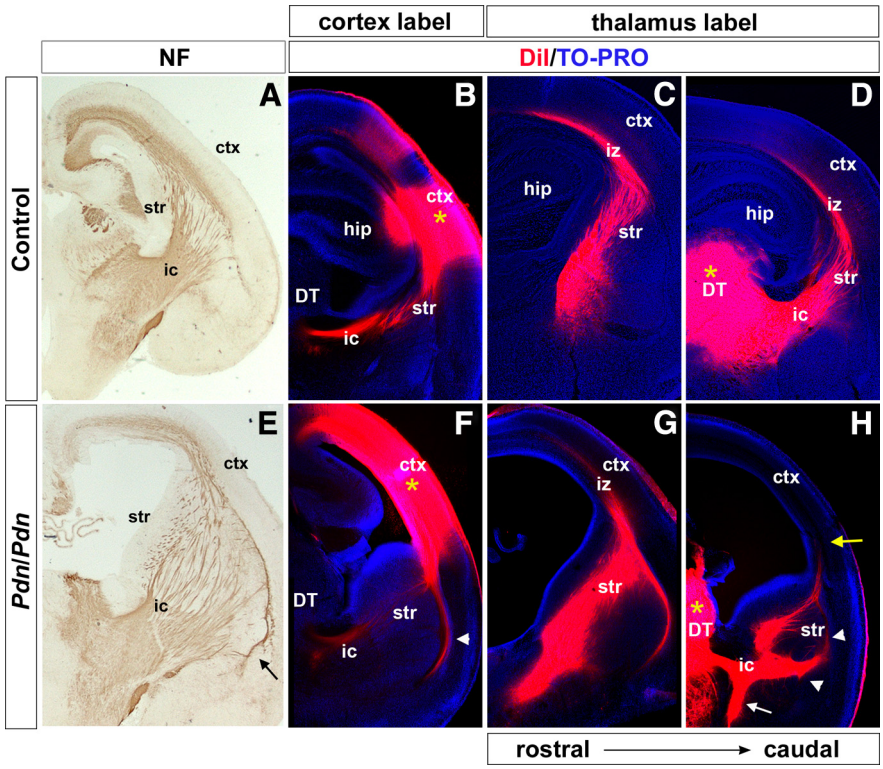

Figure 7. Axon guidance defects in the P0 *Pdn/Pdn* brain. ***A–H***, Coronal sections through the brain of control (***A–D***) and *Pdn/Pdn* (***E–H***) newborn animals. ***A***, ***E***, Neurofilament staining shows a disorganized striatum (str) and an ectopic axon bundle running along the PSPB (arrow). ***B***, ***F***, DiI injection (asterisk) into the cortex (ctx) revealed fewer axon fibers in the striatum and ectopic axons deflected at the PSPB (arrowhead). ***C***, ***D***, ***G***, ***H***, Thalamic DiI injections (asterisk) revealed trajectories of TCAs. In the mutant, some TCAs enter the cortex rostrally but an ectopic axon bundle runs along the PSPB (***G***). Caudally, an ectopic axon bundle runs ventrally in the basal ganglia (white arrow) whereas other fiber bundles leave the internal capsule (ic) prematurely and directly project toward the PSPB (***H***, arrowheads). DT, Dorsal thalamus; hip, hippocampus; iz, intermediate zone.

smaller in *Pdn/Pdn* embryos (Fig. 6*D*,*H*). This altered morphology may also cause subtle changes in the expression of axon guidance molecules important for the navigation of thalamocortical and corticothalamic axons through the ventral telencephalon (supplemental Fig. 2, available at www.jneurosci.org as supplemental material). Together, these results suggest an abnormal organization of the MGE mantle zone having ectopic Isl1/2$^+$ cells adjacent to an abnormally small globus pallidus.

The corticothalamic and thalamocortical tracts develop abnormally in *Pdn/Pdn* mutant mice

Next, we analyzed the development of the thalamocortical and corticothalamic tracts in *Pdn/Pdn* mutants. In control newborn (P0) brains, neurofilament (NF) immunostaining showed thalamocortical and corticofugal axons running through the VT, loosely organized within the striatum but more densely packed in the internal capsule (Fig. 7*A*). NF staining showed the presence of these tracts in *Pdn/Pdn* animals but axons in the striatum appear disorganized, with some axons running in several abnormal directions (Fig. 7*E*). Moreover, a thick axon bundle runs along the PSPB.

To further characterize the development of these tracts, we injected DiI crystals into the cortex and thalamus of control and *Pdn/Pdn* P0 brains. In control animals, thalamocortical and corticothalamic axons have completed their journey to their target regions in the cortex and dorsal thalamus, respectively. DiI injections in the cortex and thalamus reveal the full length of the two tracts (Fig. 7*B–D*). Axons are arranged in approximately parallel bundles in the striatum and are highly fasciculated in the internal capsule. In contrast, DiI injections into P0 mutant brains showed several abnormalities. Although DiI injected into the cortex diffuses into the dorsal thalamus, indicating that some *Pdn/Pdn* cortical and/or thalamic axons reach their final targets, fewer axons are labeled in the internal capsule (Fig. 7*F*) and the most strongly labeled bundle runs along the PSPB (Fig. 7*F*). DiI injections into the thalamus also revealed abnormal axonal trajectories, which vary along the rostral/caudal axis. Rostrally, labeled axons channel through the internal capsule, appear more disorganized in the striatum, and are present in a bundle running along the PSPB (Fig. 7*G*). Caudally, labeled axons are also seen traversing the internal capsule, but abnormal bundles are seen growing ventrally through the globus pallidus toward the amygdala (Fig. 7*H*, white arrow) and projecting directly laterally between the internal capsule and the PSPB with a dorsal turn toward the cortex. Abnormally, few labeled axons enter the cortex, particularly caudally (Fig. 7*H*). Together, these analyses indicate a severe reduction in numbers of corticothalamic axons, many of which run along the PSPB, and a major misrouting of many thalamocortical axons in the VT of P0 *Pdn/Pdn* mutants.

To gain insights into the development of these defects, NF staining was performed on E14.5 control and *Pdn/Pdn* brains. NF$^+$ axons are present in the developing thalamus, VT, and cortex of control embryos. The internal capsule contains a high density of NF$^+$ axons whereas the striatum has more loosely organized axons (Fig. 8*A*). *Pdn/Pdn* embryos have NF$^+$ axons in the thalamus and VT (Fig. 8*B*), but axons run in a more disorganized manner in dorsal regions of the LGE and there are no NF$^+$ axons in the mutant neocortex. NF$^+$ axons stop in the VT before reaching the PSPB with no axons coming from or arriving at the cortex.

The trajectories of thalamocortical and corticothalamic axons were investigated by DiI injections into the E14.5 cortex and thalamus. In control brains, thalamocortical and corticothalamic axons reach the VT around E13.5/E14.5 (López-Bendito and Molnár, 2003). While cortical axons are just starting to cross the PSPB at E14.5, thalamocortical axons have already penetrated the MGE, channeled through the internal capsule, and started to enter the developing cortex. In controls, therefore, cortical DiI injections anterogradely label the corticothalamic tract and retrogradely label the thalamocortical tract (Fig. 8*C*,*E*), whereas E14.5 dorsal thalamic DiI injections reveal anterogradely labeled thalamocortical axons only (Fig. 8*G*,*I*). In *Pdn/Pdn* embryos, cortical DiI injections showed no labeled axons entering or leaving the cortex (Fig. 8*D*,*F*). Thalamic axons pass over the diencephalic/telencephalic boundary and funnel through the internal capsule but subsequently defasciculate and some axons project ventrally to the amygdaloid region (Fig. 8*H*). This ventral deflection was more pronounced at caudal levels (Fig. 8*J*). These results indicate that the corticothalamic and thalamocortical defects ob-

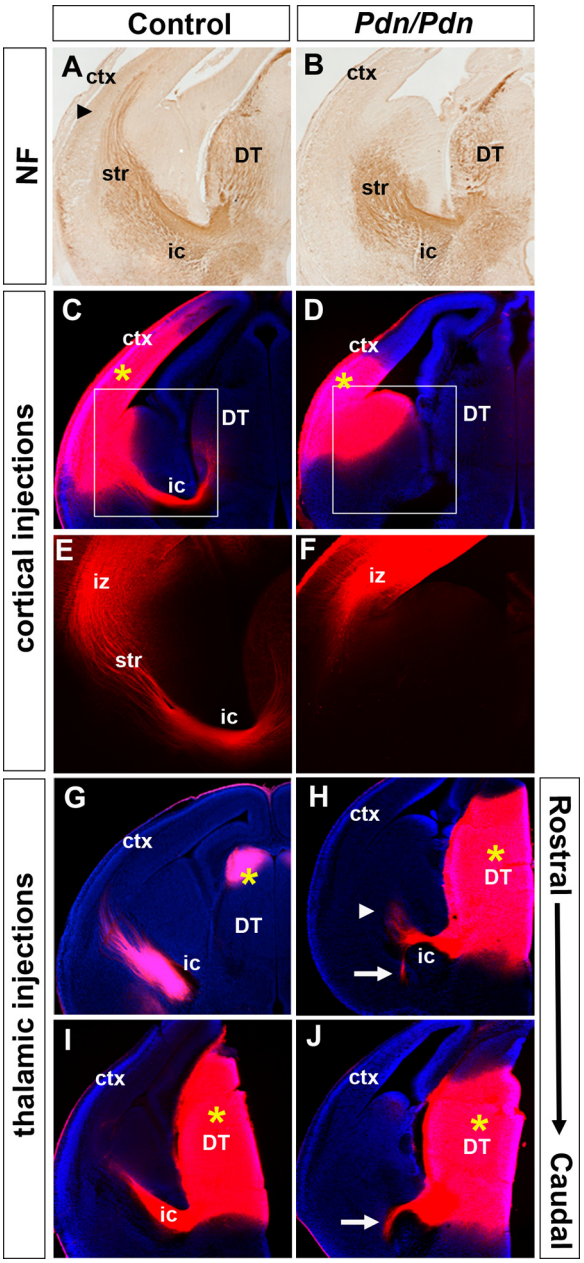

Figure 8. Development of the corticothalamic and thalamocortical tract. ***A–J***, Coronal sections through the brains of control (***A***, ***C***, ***E***, ***G***, ***I***) and *Pdn/Pdn* (***B***, ***D***, ***F***, ***H***, ***J***) E14.5 embryos. ***A***, Neurofilament staining reveals axons in the cortex (ctx, arrowhead). ***B***, The mutant neocortex lacks neurofilament staining and TCAs have not reached the cortex yet. ***C–F***, Cortical DiI injections (*) reveal the corticothalamic and thalamocortical tracts in control embryos (***C***, ***E***) whereas CTAs fail to enter the VT in *Pdn/Pdn* embryos (***D***, ***F***). ***G–J***, Thalamic DiI injections (*) show TCAs having migrated through the VT along the internal capsule (ic). In the rostral forebrain, some mutant TCAs enter the internal capsule but soon defasciculate (arrowhead), whereas others project ventrally toward the amygdala (arrow) (***G***, ***H***). This ventral deflection is more pronounced caudally (***I***, ***J***). str, Striatum.

served at P0 have their origin at the time when these tracts are forming.

Golli-tau-GFP reveals cortical axon pathfinding defects

Results from DiI analysis indicated severe pathfinding defects of corticofugal axons in *Pdn/Pdn* mutants. To examine corticothalamic axons in isolation, we used the *Golli tau-green fluorescent protein* (*τGFP*) mouse line (Jacobs et al., 2007), in which the *golli* promoter element of the myelin basic protein gene drives the expression of a τGFP fusion protein in subplate and deep cortical neurons and labels their cell bodies and axons. In E14.5 control embryos, GFP$^+$ axons were detected in the intermediate zone of the cortex and in the dorsal-most part of the LGE (Fig. 9*A*). GFP immunostaining in combination with immunofluorescence for Glast, which labels glial fascicles at the PSPB, confirmed that corticothalamic axons have just passed over the PSPB (Fig. 9*A*). Two days later, these axons have navigated through the internal capsule (Fig. 9*B*). In *Pdn/Pdn*;*Golli tau-GFP* brains, GFP$^+$ neurons are formed normally but we could not detect any GFP$^+$ axons projecting over the PSPB at E14.5 and at E16.5. Instead, a GFP$^+$ axon bundle runs along the PSPB (Fig. 9*C*,*D*). In P0 control animals, GFP is expressed in the cell bodies and axons of cortical neurons (Fig. 9*E*,*F*), in particular in layers 5 and 6 and in subplate neurons (Jacobs et al., 2007). At this stage, corticofugal GFP$^+$ axons have reached the dorsal thalamus (Fig. 9*F*). In P0 *Pdn/Pdn Golli τGFP* animals, some *Pdn/Pdn* GFP$^+$ corticothalamic axons extend into the diencephalon, but none reach the dorsal thalamus and many make abnormal sharp turns in the striatum (Fig. 9*G*,*H*). These findings indicate a developmental delay of the corticothalamic tract and pathfinding errors in the VT.

The *Pdn/Pdn* VT is compromised in its ability to guide thalamocortical and corticofugal axons

It is likely that the severe defects in *Pdn/Pdn* VT are a major cause of the corticofugal and thalamocortical axonal defects in this region. This is strengthened by our finding that, although the *Pdn/Pdn* cortex is thinner, neither thalamus nor cortex shows obvious abnormalities in their patterns of expression of several maker genes (supplemental Figs. 3–5, available at www.jneurosci.org as supplemental material). Cortical layers appear to form relatively normally and corticofugal neurons are specified (supplemental Figs. 4, 5, available at www.jneurosci.org as supplemental material). Defects in cortical arealization are confined to the motor cortex, which is decreased in size (supplemental Fig. 6, available at www.jneurosci.org as supplemental material), probably due to a ventralization of the rostrodorsal telencephalon (Kuschel et al., 2003), but somatosensory and visual cortex are formed normally (supplemental Fig. 6, available at www.jneurosci.org as supplemental material). In addition, non-neural cell populations such as oligodendrocytes are present normally in the *Pdn/Pdn* cortex (supplemental Fig. 7, available at www.jneurosci.org as supplemental material). Nevertheless, since reduced *Gli3* levels in thalamus and/or cortex might explain the abnormal development of thalamocortical and/or corticothalamic projections, we used a recently developed *in vitro* transplantation assay (López-Bendito et al., 2006) to test directly the ability of the *Pdn/Pdn* VT to guide thalamocortical axons. *Pdn* mutants were crossed with mice ubiquitously expressing a τGFP fusion protein (Pratt et al., 2000). Dorsal thalamic tissue from E13.5 GFP$^+$ embryos was transplanted into the preoptic area of age-matched GFP$^-$ embryos, from where thalamic axons can enter the permissive corridor in the MGE (López-Bendito et al., 2006). Transplantation of control;GFP$^+$ thalamic tissue into control preoptic area led to axon outgrowth from the transplant toward the neocortex ($n = 8$ of 9) (Fig. 10*A–D*). Most thalamic axons migrated in the internal capsule ($n = 8$ of 9) and, in a few cases, axons crossed the LGE and reached the cortex ($n = 3$ of 9). Some axons also grew in the external capsule ($n = 4$ of 9), as observed previously (López-Bendito et al., 2006). After transplantation of *Pdn/Pdn*;*GFP*$^+$ thalamus into control preoptic area, axons also migrated in the internal capsule ($n = 7$ of 9) and in the external capsule ($n = 3$ of

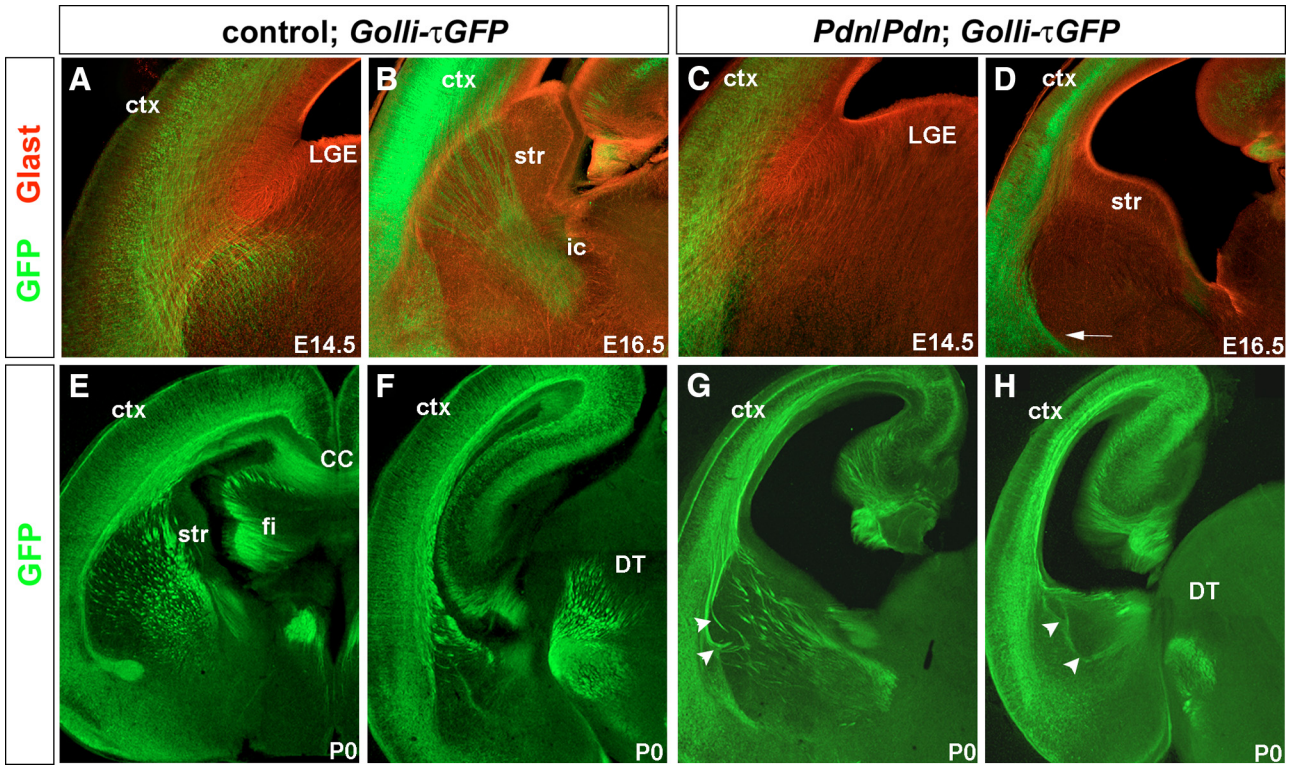

Figure 9. The *Golli-τGFP* transgene reveals pathfinding defects of corticofugal axons. ***A–H***, Coronal sections through the brains of E14.5 (***A***, ***C***) and E16.5 (***B***, ***D***) embryos and P0 (***E–H***) control and *Pdn/Pdn* animals carrying the *Golli-τGFP* transgene. ***A***, ***B***, GFP immunofluorescence shows cortical axons crossing the PSPB (E14.5) and penetrating the VT (E16.5). Glast immunofluorescence labels glial fascicles at the PSPB. ***C***, ***D***, *Pdn/Pdn* corticofugal axons fail to enter the VT but project along the PSPB (***C***, ***D***, arrow). ***E***, ***F***, In newborn control animals, GFP is expressed in the cell bodies and axons of layer 5 and 6 neurons and in subplate neurons. GFP$^+$ axons have reached the dorsal thalamus. ***G***, ***H***, Few *Pdn/Pdn* GFP$^+$ corticothalamic axons extend into the diencephalon but have not reached the thalamus. Many axons take abnormal routes in the striatum (str) whereas others project along the PSPB. DT, Dorsal thalamus; ctx, cortex; ic, internal capsule; CC, corpus callosum; fi, fimbria.

9) (Fig. 10*E*,*F*), although a few axons grew along the ventral edge of the explant ($n = 4$ of 9), a path which was not observed in control experiments. When we transplanted control;GFP$^+$ thalamus into the preoptic area of *Pdn/Pdn*;GFP$^-$ embryos, we observed thalamic axons growing into the mutant VT in a disorganized manner and it was never possible to recognize pathways reminiscent of the internal or external capsule ($n = 10$ of 10) (Fig. 10*G*,*H*). Some axons also projected along the ventral edge of the explant ($n = 6$ of 10). These findings indicate that the *Pdn/Pdn* mutant VT lacks an intrinsic ability to guide thalamic axons normally. Our findings also indicate that some mutant thalamic axons might have defects in their ability to follow guidance cues provided by the wild-type VT.

Finally, we used a similar transplantation assay to test the ability of *Pdn/Pdn* corticofugal axons to cross the PSPB and enter the striatum. For this purpose, cortical tissue from E16.5 GFP$^+$ embryos was transplanted into the cortex of age-matched GFP$^-$ embryos, from where cortical axons can enter the intermediate zone and grow toward the ventral telencephalon. Transplantation of control;GFP$^+$ cortical tissue into control cortex led to axon outgrowth from the transplant into the striatum ($n = 10$ of 10) (Fig. 10*I*). When we transplanted *Pdn/Pdn*;GFP$^+$ cortex into control cortex, we similarly observed GFP$^+$ axons penetrating the ventral telencephalon ($n = 16$ of 16) (Fig. 10*J*). In contrast, corticofugal axons do not enter the striatum but migrate along the PSPB after transplantation of control;GFP$^+$ thalamus into the cortex of *Pdn/Pdn*;GFP$^-$ embryos ($n = 5$ of 5) (Fig. 10*K*), suggesting that the *Pdn/Pdn* ventral telencephalon has lost its ability to guide corticofugal axons into the striatum.

Discussion

In this study, we show that *Pdn/Pdn* embryos have an overall reduction of *Gli3* expression levels, but graded *Gli3* expression in the VT remains. This reduced *Gli3* expression coincides with an upregulation of *Shh* expression in the VT and an extension of Shh signaling into the LGE. *Pdn/Pdn* mutants have severe patterning defects in the ventral telencephalon. Although the MGE mantle zone becomes disorganized, the LGE is most affected, showing growth and regionalization defects that have effects on the pathfinding of thalamocortical and corticothalamic axons.

Reduced *Gli3* expression levels alter patterning of the VT

The function of *Gli3* during the development of the ventral telencephalon is poorly understood. In the *Gli3* hypomorphic mutation *Pdn*, the PSPB is shifted dorsally and is less well defined. Moreover, the LGE is partially ventralized at caudal levels and the LGE mantle is much reduced in thickness due to an elongation of the cell cycle of LGE progenitors, which leads to a decreased production of LGE neurons. Moreover, in newborn *Pdn* mutants, these early embryonic changes are consistent with an expansion of striatal projection neurons derived from the ventral LGE (supplemental Fig. 8, available at www.jneurosci.org as supplemental material). Collectively, these phenotypes suggest that normal LGE development is highly sensitive to changes in *Gli3* expression levels consistent with its position between the dorsal telencephalon, in which the Gli3 repressor predominates, and the MGE with high levels of Gli3 activator (Fotaki et al., 2006). The relative severity of the LGE phenotypes in *Pdn/Pdn* mutants is also in contrast to mice lacking *Gli3* completely. These animals show ventral telencephalic growth and differentiation defects

(Yu et al., 2009a), but the major defects are in the dorsal telencephalon. Therefore, it appears that *Gli3* levels in the LGE of normal mice might be close to a threshold required for normal development whereas *Gli3* levels in the dorsal telencephalon might be well above such a threshold.

Interestingly, the *Pdn* mutation leads to upregulation of *Shh* expression and signaling in the ventral telencephalon, suggesting that the phenotypes described above are linked to this upregulation. Their occurrence coincides with the onset of altered Shh signaling at E10.5 (Ueta et al., 2008) and the regionalization and growth defects in the *Pdn*/*Pdn* ventral telencephalon are consistent with known roles of Shh in regulating ventral telencephalic gene expression (Shimamura and Rubenstein, 1997; Rallu et al., 2002; Fuccillo et al., 2004; Xu et al., 2005; Yu et al., 2009b) and the expression of cell cycle regulators in neural tissues (Kenney and Rowitch, 2000; Ishibashi and McMahon, 2002; Kenney et al., 2003; Oliver et al., 2003; Lobjois et al., 2004; Cayuso et al., 2006; Alvarez-Medina et al., 2009). Also, ectopic Shh expression in the dorsal spinal cord results in reduced neurogenesis (Rowitch et al., 1999). These findings are therefore in line with previous analyses that showed the antagonism between *Shh* and *Gli3* to be an important determinant of ventral telencephalic patterning (Rallu et al., 2002; Rash and Grove, 2007). This antagonism involves interactions at multiple levels. Shh signaling inhibits the proteolytic processing of Gli3 into its repressor form, which negatively controls the expression of Shh target genes. Also, *Gli3* expression is downregulated in neural cells close to a Shh source. Here, we extend these findings by showing that *Gli3* in turn negatively regulates *Shh* expression in the ventral telencephalon. A more pronounced, but VT-restricted, increase in *Shh* expression is also found in Xt^J/Xt^J mutants (K.H.T. and T.T., unpublished data). These reciprocal interactions therefore appear to be part of a complex feedback mechanism that ensures the production of correct *Gli3* repressor and Shh signaling levels. Finally, the *Shh*/*Gli3* antagonism has been inferred from the analyses of loss-of-function mutations, which indicates an absolute requirement for both genes in VT patterning (Rallu et al., 2002; Rash and Grove, 2007). Changing *Gli3* expression levels and thereby the amount and extent of Shh signaling as in *Pdn*/*Pdn* mutants also has severe consequences on telencephalic development, emphasizing the importance of relative *Gli3* and *Shh* expression levels and supporting a model where opposite gradients of Gli3 repressor and Shh signaling control patterning of the ventral telencephalon.

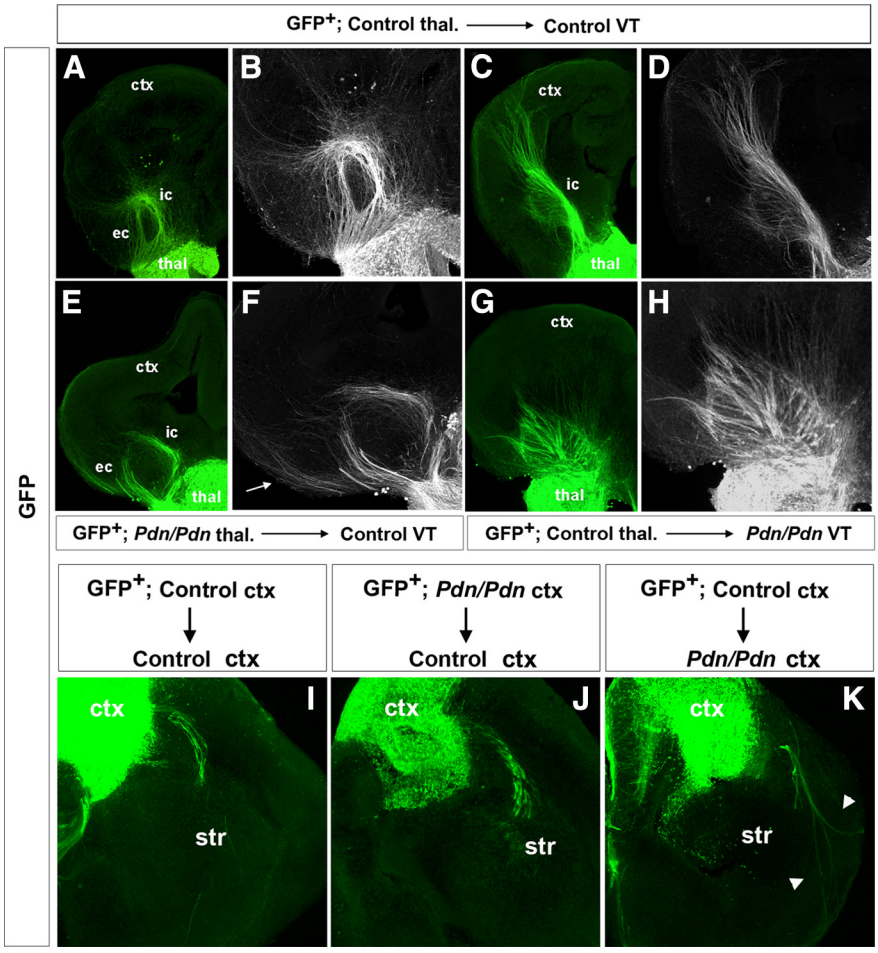

Figure 10. The *Pdn* mutant VT lacks the ability to guide thalamic and cortical axons. ***A–D***, Transplantation of control τGFP$^+$ thalamic tissue into the preoptic area of control embryos. Thalamic axons (thal) grow through the VT via the internal (ic) and the external (ec) capsule and enter the cortex (ctx; ***C***, ***D***). ***E***, ***F***, Transplantation of *Pdn*/*Pdn* τGFP$^+$ thalamic tissue into the preoptic area of control embryos. Mutant thalamic axons grow into the VT via the internal and external capsules, but some axons project along the edge of the transplant (***F***, arrow). ***G***, ***H***, Transplantation of control τGFP$^+$ thalamic tissue into the preoptic area of *Pdn*/*Pdn* embryos. Thalamic axons grow into the VT in a disorganized manner. ***I***, Transplantation of control τGFP$^+$ cortical tissue into the frontal cortex of control embryos. Cortical axons grow along the intermediate zone until they cross the PSPB and enter the striatum (str). ***J***, Transplantation of *Pdn*/*Pdn* τGFP$^+$ cortical tissue into the frontal cortex of control embryos. Mutant cortical axons grow in the control intermediate zone and cross the PSPB entering the striatum. ***K***, Transplantation of control τGFP$^+$ cortical tissue into the frontal cortex of *Pdn*/*Pdn* embryos. GFP$^+$ cortical axons grow into mutant cortex in a disorganized manner, projecting away from or along the PSPB (arrowheads).

Axon guidance defects in *Pdn*/*Pdn* mutants result from early patterning defects

The ventral telencephalon gives rise to multiple neuronal and glial cell types and plays a major role in the guidance of TCAs and CTAs. Although the *Pdn*/*Pdn* ventral telencephalon still produces these cell types (Fig. 6; supplemental Figs. 7 and 8, available at www.jneurosci.org as supplemental material), its axon guidance capability is severely compromised. We showed that thalamocortical axons are capable of penetrating the VT but then project in abnormal directions, either into the amygdaloid region at caudal levels or prematurely exiting the internal capsule at rostral levels. Several lines of evidence indicate that defects in the VT play a major role in the development of these abnormalities. Patterning of the dorsal thalamus is not affected in *Pdn*/*Pdn* mutants. In contrast, the mantle zone of the MGE is disorganized and shows subtle changes in the expression patterns of axon guidance molecules (supplemental Fig. 2, available at www.jneurosci.org as supplemental material). These alterations may be caused by changes in the morphology of the *Pdn*/*Pdn* ventral telencephalon and are unlikely to explain the severe TCA pathfinding defects. Moreover, although the permissive corridor forms in the mutant, the globus pallidus, which is nonpermissive for thalamocortical axons, is reduced in size, in particular in its medial extent. In-

stead, this medial MGE region, which lacks *Nkx2.1* expression in *Pdn*/*Pdn* embryos, contains numerous Isl1/2$^+$ cells. Since Isl1/2$^+$ corridor cells are capable of guiding TCAs through the otherwise nonpermissive environment of the MGE (López-Bendito et al., 2006), the scattered Isl1/2$^+$ cells might enable TCAs to enter the ventromedial MGE or leave the internal capsule prematurely. This scenario is also supported by our transplantation assay. *Pdn* mutant thalamic axons are capable of responding to ventral telencephalic guidance cues after transplantation into the preoptic area of control embryos, although some mutant axons project abnormally along the edge of the transplant, indicating some intrinsic defects. In turn, transplantation of wild-type thalamic tissue into the *Pdn*/*Pdn* preoptic area led to the disordered growth of TCAs into the host ventral telencephalon, strongly suggesting that the mutant VT is compromised in its ability to guide thalamic axons through the MGE. Together, these findings provide strong evidence for a major role of ventral telencephalic patterning defects in the development of the axon guidance defects in *Pdn* mutants.

In addition, corticofugal axons also showed severe pathfinding defects. Only a few corticothalamic axons project toward the diencephalon. DiI labeling and the use of the Golli-τGFP transgene indicate that their entry into the LGE is delayed by several days. Instead, many axons project along the PSPB, a pattern frequently observed after perturbation of early corticothalamic development (Jones et al., 2002). Several lines of evidence argue against a major involvement of the cortex in the development of this phenotype. The overall organization of the *Pdn*/*Pdn* cortex appears largely unaffected with subtle differences in cortical arealization, which are unlikely to explain the severe pathfinding defects of *Pdn*/*Pdn* corticofugal axons. More importantly, our transplantation assay clearly showed that *Pdn*/*Pdn* cortical axons can correctly navigate into the ventral telencephalon in a wild-type environment (Fig. 10).

Guidance of CTAs across the PSPB is thought to involve a transient population of pioneer neurons located in the LGE (Métin and Godement, 1996). Interestingly, the *Pdn* mutation represents the first known mutation to affect the development of these pioneers. In the absence of molecular markers, retrograde DiI labeling is the only method to identify these pioneer neurons, but it failed to label their projections; however, a similar population of pioneer neurons in the MGE is present in *Pdn*/*Pdn* embryos. LGE pioneers and their projections could also not be labeled by later (E14.5) DiI injections (Fig. 8*F*) into the cortex, arguing against a delay in their development. These findings therefore suggest either the absence of these neurons or a failure to project their axons toward the cortex. This defect might be explained by the partial ventralization of the caudal LGE and/or by the reduced neurogenesis in the LGE. Alternatively, the dorsal shift of the PSPB might interfere with the projection of these neurons as they might be separated from attractive guidance cues emanating from the cortex (López-Bendito et al., 2006). Given the known role of pioneer neurons in the development of forebrain axonal connections (McConnell et al., 1989; De Carlos and O'Leary, 1992; Supèr et al., 1998; Lakhina et al., 2007; Piper et al., 2009), defective LGE pioneer development in *Pdn*/*Pdn* embryos provides a strong explanation for the delay of CTAs to cross the PSPB. In addition, the defective formation of the PSPB might provide an alternative, not mutually exclusive, explanation for the navigation defects of CTAs (Molnár and Blakemore, 1995a; Molnár and Butler, 2002). However, the finding that corticofugal axons penetrate the ventral telencephalon in P0 mutants suggests that the LGE pioneers might be important for the correct timing of crossing and the later-arriving thalamocortical axons might guide corticothalamic axons across the PSPB (Molnár and Blakemore, 1995b).

Our study provides strong evidence that correct levels of *Gli3* expression are required for normal patterning of the VT and for the development of its axon guidance capabilities. This analysis emphasizes the link between early patterning and axon pathfinding in the developing forebrain and demonstrates a previous unknown role for *Gli3* in axonal development.

References

Alvarez-Medina R, Le Dreau G, Ros M, Martí E (2009) Hedgehog activation is required upstream of Wnt signalling to control neural progenitor proliferation. Development 136:3301–3309.

Aoto K, Nishimura T, Eto K, Motoyama J (2002) Mouse GLI3 regulates Fgf8 expression and apoptosis in the developing neural tube, face, and limb bud. Dev Biol 251:320–332.

Bulfone A, Puelles L, Porteus MH, Frohman MA, Martin GR, Rubenstein JL (1993) Spatially restricted expression of Dlx-1, Dlx-2 (Tes-1), Gbx-2, and Wnt-3 in the embryonic day 12.5 mouse forebrain defines potential transverse and longitudinal segmental boundaries. J Neurosci 13:3155–3172.

Cayuso J, Ulloa F, Cox B, Briscoe J, Martí E (2006) The Sonic hedgehog pathway independently controls the patterning, proliferation and survival of neuroepithelial cells by regulating Gli activity. Development 133:517–528.

Chiang C, Litingtung Y, Lee E, Young KE, Corden JL, Westphal H, Beachy PA (1996) Cyclopia and defective axial patterning in mice lacking Sonic hedgehog gene function. Nature 383:407–413.

De Carlos JA, O'Leary DD (1992) Growth and targeting of subplate axons and establishment of major cortical pathways. J Neurosci 12:1194–1211.

Echelard Y, Epstein DJ, St-Jacques B, Shen L, Mohler J, McMahon JA, McMahon AP (1993) Sonic hedgehog, a member of a family of putative signaling molecules, is implicated in the regulation of CNS polarity. Cell 75:1417–1430.

Ericson J, Muhr J, Placzek M, Lints T, Jessell TM, Edlund T (1995) Sonic hedgehog induces the differentiation of ventral forebrain neurons: a common signal for ventral patterning within the neural tube. Cell 81:747–756.

Flames N, Pla R, Gelman DM, Rubenstein JL, Puelles L, Marín O (2007) Delineation of multiple subpallial progenitor domains by the combinatorial expression of transcriptional codes. J Neurosci 27:9682–9695.

Fotaki V, Yu T, Zaki PA, Mason JO, Price DJ (2006) Abnormal positioning of diencephalic cell types in neocortical tissue in the dorsal telencephalon of mice lacking functional Gli3. J Neurosci 26:9282–9292.

Friedrichs M, Larralde O, Skutella T, Theil T (2008) Lamination of the cerebral cortex is disturbed in Gli3 mutant mice. Dev Biol 318:203–214.

Fuccillo M, Rallu M, McMahon AP, Fishell G (2004) Temporal requirement for hedgehog signaling in ventral telencephalic patterning. Development 131:5031–5040.

Gaiano N, Kohtz JD, Turnbull DH, Fishell G (1999) A method for rapid gain-of-function studies in the mouse embryonic nervous system. Nat Neurosci 2:812–819.

Goodrich LV, Johnson RL, Milenkovic L, McMahon JA, Scott MP (1996) Conservation of the hedgehog/patched signaling pathway from flies to mice: induction of a mouse patched gene by Hedgehog. Genes Dev 10:301–312.

Grove EA, Tole S, Limon J, Yip L, Ragsdale CW (1998) The hem of the embryonic cerebral cortex is defined by the expression of multiple Wnt genes and is compromised in Gli3-deficient mice. Development 125:2315–2325.

Hanashima C, Fernandes M, Hebert JM, Fishell G (2007) The role of Foxg1 and dorsal midline signaling in the generation of Cajal-Retzius subtypes. J Neurosci 27:11103–11111.

Hayasaka I, Nakatsuka T, Fujii T, Naruse I, Oda S (1980) *Polydactyly Nagoya*, *Pdn*: a new mutant gene in the mouse. Jikken Dobutsu 29:391–395.

Hui CC, Slusarski D, Platt KA, Holmgren R, Joyner AL (1994) Expression of three mouse homologs of the *Drosophila* segment polarity gene cubitus interruptus, Gli, Gli-2, and Gli-3, in ectoderm- and mesoderm-derived tissues suggests multiple roles during postimplantation development. Dev Biol 162:402–413.

Ishibashi M, McMahon AP (2002) A sonic hedgehog-dependent signaling

relay regulates growth of diencephalic and mesencephalic primordia in the early mouse embryo. Development 129:4807–4819.
Jacobs EC, Campagnoni C, Kampf K, Reyes SD, Kalra V, Handley V, Xie YY, Hong-Hu Y, Spreur V, Fisher RS, Campagnoni AT (2007) Visualization of corticofugal projections during early cortical development in a tau-GFP-transgenic mouse. Eur J Neurosci 25:17–30.
Jones L, López-Bendito G, Gruss P, Stoykova A, Molnár Z (2002) Pax6 is required for the normal development of the forebrain axonal connections. Development 129:5041–5052.
Kenney AM, Rowitch DH (2000) Sonic hedgehog promotes G(1) cyclin expression and sustained cell cycle progression in mammalian neuronal precursors. Mol Cell Biol 20:9055–9067.
Kenney AM, Cole MD, Rowitch DH (2003) Nmyc upregulation by sonic hedgehog signaling promotes proliferation in developing cerebellar granule neuron precursors. Development 130:15–28.
Kohtz JD, Baker DP, Corte G, Fishell G (1998) Regionalization within the mammalian telencephalon is mediated by changes in responsiveness to Sonic Hedgehog. Development 125:5079–5089.
Kuschel S, Rüther U, Theil T (2003) A disrupted balance between Bmp/Wnt and Fgf signaling underlies the ventralization of the Gli3 mutant telencephalon. Dev Biol 260:484–495.
Lakhina V, Falnikar A, Bhatnagar L, Tole S (2007) Early thalamocortical tract guidance and topographic sorting of thalamic projections requires LIM-homeodomain gene Lhx2. Dev Biol 306:703–713.
Lazzaro D, Price M, de Felice M, Di Lauro R (1991) The transcription factor TTF-1 is expressed at the onset of thyroid and lung morphogenesis and in restricted regions of the foetal brain. Development 113:1093–1104.
Lee J, Platt KA, Censullo P, Ruiz i Altaba A (1997) Gli1 is a target of Sonic hedgehog that induces ventral neural tube development. Development 124:2537–2552.
Lobjois V, Benazeraf B, Bertrand N, Medevielle F, Pituello F (2004) Specific regulation of cyclins D1 and D2 by FGF and Shh signaling coordinates cell cycle progression, patterning, and differentiation during early steps of spinal cord development. Dev Biol 273:195–209.
López-Bendito G, Molnár Z (2003) Thalamocortical development: how are we going to get there? Nat Rev Neurosci 4:276–289.
López-Bendito G, Cautinat A, Sánchez JA, Bielle F, Flames N, Garratt AN, Talmage DA, Role LW, Charnay P, Marín O, Garel S (2006) Tangential neuronal migration controls axon guidance: a role for neuregulin-1 in thalamocortical axon navigation. Cell 125:127–142.
Martynoga B, Morrison H, Price DJ, Mason JO (2005) Foxg1 is required for specification of ventral telencephalon and region-specific regulation of dorsal telencephalic precursor proliferation and apoptosis. Dev Biol 283:113–127.
McConnell SK, Ghosh A, Shatz CJ (1989) Subplate neurons pioneer the first axon pathway from the cerebral cortex. Science 245:978–982.
Métin C, Godement P (1996) The ganglionic eminence may be an intermediate target for corticofugal and thalamocortical axons. J Neurosci 16:3219–3235.
Molnár Z, Blakemore C (1995a) Guidance of thalamocortical innervation. Ciba Found Symp 193:127–149.
Molnár Z, Blakemore C (1995b) How do thalamic axons find their way to the cortex? Trends Neurosci 18:389–397.
Molnár Z, Butler AB (2002) The corticostriatal junction: a crucial region for forebrain development and evolution. Bioessays 24:530–541.
Molnár Z, Adams R, Blakemore C (1998) Mechanisms underlying the early establishment of thalamocortical connections in the rat. J Neurosci 18:5723–5745.
Oliver G, Mailhos A, Wehr R, Copeland NG, Jenkins NA, Gruss P (1995) Six3, a murine homologue of the sine oculis gene, demarcates the most anterior border of the developing neural plate and is expressed during eye development. Development 121:4045–4055.
Oliver TG, Grasfeder LL, Carroll AL, Kaiser C, Gillingham CL, Lin SM, Wickramasinghe R, Scott MP, Wechsler-Reya RJ (2003) Transcriptional profiling of the Sonic hedgehog response: a critical role for *N*-myc in proliferation of neuronal precursors. Proc Natl Acad Sci U S A 100:7331–7336.
Piper M, Plachez C, Zalucki O, Fothergill T, Goudreau G, Erzurumlu R, Gu C, Richards LJ (2009) Neuropilin 1-Sema signaling regulates crossing of cingulate pioneering axons during development of the corpus callosum. Cereb Cortex 19 [Suppl 1]:i11–i21.
Pratt T, Sharp L, Nichols J, Price DJ, Mason JO (2000) Embryonic stem cells and transgenic mice ubiquitously expressing a tau-tagged green fluorescent protein. Dev Biol 228:19–28.
Qiu M, Shimamura K, Sussel L, Chen S, Rubenstein JL (1998) Control of anteroposterior and dorsoventral domains of Nkx-6.1 gene expression relative to other Nkx genes during vertebrate CNS development. Mech Dev 72:77–88.
Quinn JC, Molinek M, Mason JO, Price DJ (2009) Gli3 is required autonomously for dorsal telencephalic cells to adopt appropriate fates during embryonic forebrain development. Dev Biol 327:204–215.
Rallu M, Machold R, Gaiano N, Corbin JG, McMahon AP, Fishell G (2002) Dorsoventral patterning is established in the telencephalon of mutants lacking both Gli3 and Hedgehog signaling. Development 129:4963–4974.
Rash BG, Grove EA (2007) Patterning the dorsal telencephalon: a role for sonic hedgehog? J Neurosci 27:11595–11603.
Rowitch DH, St.-Jacques B, Lee SMK, Flax JD, Snyder EY, McMahon AP (1999) Sonic hedgehog regulates proliferation and inhibits differentiation of CNS precursor cells. J Neurosci 19:8954–8965.
Shimamura K, Rubenstein JL (1997) Inductive interactions direct early regionalization of the mouse forebrain. Development 124:2709–2718.
Supèr H, Soriano E, Uylings HB (1998) The functions of the preplate in development and evolution of the neocortex and hippocampus. Brain Res Brain Res Rev 27:40–64.
Theil T (2005) Gli3 is required for the specification and differentiation of preplate neurons. Dev Biol 286:559–571.
Theil T, Alvarez-Bolado G, Walter A, Rüther U (1999) Gli3 is required for *Emx* gene expression during dorsal telencephalon development. Development 126:3561–3571.
Thien H, Rüther U (1999) The mouse mutation *Pdn* (*Polydactyly Nagoya*) is caused by the integration of a retrotransposon into the Gli3 gene. Mamm Genome 10:205–209.
Tole S, Ragsdale CW, Grove EA (2000) Dorsoventral patterning of the telencephalon is disrupted in the mouse mutant extra-toes(J). Dev Biol 217:254–265.
Toresson H, Potter SS, Campbell K (2000) Genetic control of dorsal-ventral identity in the telencephalon: opposing roles for Pax6 and Gsh2. Development 127:4361–4371.
Tuttle R, Nakagawa Y, Johnson JE, O'Leary DD (1999) Defects in thalamocortical axon pathfinding correlate with altered cell domains in Mash-1-deficient mice. Development 126:1903–1916.
Ueta E, Nanba E, Naruse I (2002) Integration of a transposon into the Gli3 gene in the Pdn mouse. Congenit Anom (Kyoto) 42:318–322.
Ueta E, Kurome M, Teshima Y, Kodama M, Otsuka Y, Naruse I (2008) Altered signaling pathway in the dysmorphogenesis of telencephalon in the Gli3 depressed mouse embryo, Pdn/Pdn. Congenit Anom (Kyoto) 48:74–80.
Valerius MT, Li H, Stock JL, Weinstein M, Kaur S, Singh G, Potter SS (1995) Gsh-1: a novel murine homeobox gene expressed in the central nervous system. Dev Dyn 203:337–351.
Xu Q, Wonders CP, Anderson SA (2005) Sonic hedgehog maintains the identity of cortical interneuron progenitors in the ventral telencephalon. Development 132:4987–4998.
Yu T, Fotaki V, Mason JO, Price DJ (2009a) Analysis of early ventral telencephalic defects in mice lacking functional Gli3 protein. J Comp Neurol 512:613–627.
Yu W, Wang Y, McDonnell K, Stephen D, Bai CB (2009b) Patterning of ventral telencephalon requires positive function of Gli transcription factors. Dev Biol 334:264–275.
Yun K, Potter S, Rubenstein JL (2001) Gsh2 and Pax6 play complementary roles in dorsoventral patterning of the mammalian telencephalon. Development 128:193–205.
Yun K, Garel S, Fischman S, Rubenstein JL (2003) Patterning of the lateral ganglionic eminence by the Gsh1 and Gsh2 homeobox genes regulates striatal and olfactory bulb histogenesis and the growth of axons through the basal ganglia. J Comp Neurol 461:151–165.